

Measurements Based Channel Characterization for Vehicle-to-Vehicle **Communications at Merging Lanes on Highway**

Abbas, Taimoor; Bernado, Laura; Thiel, Andreas; F. Mecklenbräuker, Christoph; Tufvesson, Fredrik

2013 IEEE 5th International Symposium on Wireless Vehicular Communications, WiVeC 2013 - Proceedings

DOI:

10.1109/wivec.2013.6698241

2013

Link to publication

Citation for published version (APA):

Abbas, T., Bernado, L., Thiel, A., F. Mecklenbräuker, C., & Tufvesson, F. (2013). Measurements Based Channel Characterization for Vehicle-to-Vehicle Communications at Merging Lanes on Highway. In 2013 IEEE 5th International Symposium on Wireless Vehicular Communications, WiVeC 2013 - Proceedings IEEE - Institute of Electrical and Électronics Engineers Inc.. https://doi.org/10.1109/wivec.2013.6698241

Total number of authors:

General rights

Unless other specific re-use rights are stated the following general rights apply: Copyright and moral rights for the publications made accessible in the public portal are retained by the authors and/or other copyright owners and it is a condition of accessing publications that users recognise and abide by the legal requirements associated with these rights

- Users may download and print one copy of any publication from the public portal for the purpose of private study
- You may not further distribute the material or use it for any profit-making activity or commercial gain
 You may freely distribute the URL identifying the publication in the public portal

Read more about Creative commons licenses: https://creativecommons.org/licenses/

If you believe that this document breaches copyright please contact us providing details, and we will remove access to the work immediately and investigate your claim.

LUND UNIVERSITY

PO Box 117 221 00 Lund +46 46-222 00 00

Download date: 02. Dec. 2025

Measurements Based Channel Characterization for Vehicle-to-Vehicle Communications at Merging Lanes on Highway

Taimoor Abbas*, Laura Bernadó[†], Andreas Thiel[‡], Christoph F. Mecklenbräuker[§], and Fredrik Tufvesson*

*Department of Electrical and Information Technology, Lund University, Lund, Sweden

[†]Forschungszentrum Telekommunikation Wien (FTW), Vienna, Austria

[‡]Delphi Deutschland GmbH, Bad Salzdetfurth, Germany

[§]Institute of Telecommunications, Vienna University of Technology, Vienna, Austria

Abstract—This paper presents results for vehicle-to-vehicle channel characterization based on measurements conducted for a merging lane scenario on a highway. We present power delay profiles as well as channel gains and analyze important propagation mechanisms to see the impact of line-of-sight (LOS) and the antenna radiation pattern on the total received power. It is found that the absence of LOS and strong scattering objects, close to the point where the ramp merges with a highway may result in poor received signal strength. The probability of dropping packets also increases where there is LOS between TX and RX but the antenna pattern is not omni-directional. A dip in the antenna pattern affects the received signal strength severely which poses a challenge for vehicle-to-vehicle communication in safety critical situations.

I. Introduction

Vehicle-to-Vehicle (V2V) communication is a challenging but fast growing technology. It has potential to enhance the road safety by supporting the driver to avoid collisions in the basic maneuvers such as crossing street intersections, changing lanes, merging on a highway, and driving safely in curves and blind turns. The significance of V2V safety applications increases further where the visual line-of-sight (LOS) is unavailable, e.g., in the situations when roads are intersecting at a certain angle on a highway, the entrance or exit ramps. The reliability of these applications highly depends on the quality of the communication link, which rely upon the properties of propagation channel. Therefore, understanding the properties of the propagation channel becomes extremely important.

A number of research outcomes have been published covering many aspects of V2V communications but to the author's best knowledge there are no measurement results available for channel characterization in merging lane scenarios. However, some theoretical and simulation based studies have been conducted in the past dealing with the merging lane situation [1]–[4], in which the merging/changing lane control algorithms and systems are discussed, and simulation results are provided to show how to avoid possible collisions. In most of the simulation studies the antennas are assumed to be isotropic, radiating equal power in all directions, and the communication range is assumed to be a circle around the TX, which is not the case in reality. The communication range depends on a number

of factors involving the antenna radiation pattern, location of the antenna on the car, the traffic density, obstacles such as buildings and vehicles, and the transmitted power.

The antenna pattern is one of the major limiting factors and to perform a realistic simulation studies it is necessary to use somewhat realistic antenna patterns.

Merging lanes occur often in highway or rural environment, this is why there are few big objects around that can contribute to increase the scattering. If the antenna pattern has a dip in the direction-of-departure (DOD) or direction-of-arrival (DOA) of LOS path, then the probability of losing the packets is high because there are no other significant scatterers to carry the signal power. Thus an antenna pattern should be designed such that it has equal gain in almost all directions or multiple antennas should be considered. To emphasize this we analyze measurements collected in merging lanes situations and present the results for this antenna-channel interaction. The directional analysis is performed using a high resolution space-alternating expectation maximization algorithm (SAGE) [5] for selected time-snapshots. Particular focus is put on the LOS component as it carries most of the received power. The DOA/DOD estimates are presented to show how antenna pattern can affect the received signal strength, when the LOS component is received at an angle where the antenna has a lower gain.

The rest of the paper is organized as follows, in section II we present the V2V measurement setup, and explain the merging lane scenarios. In section III we discuss the data analysis and results, and explain how the results have been extracted for time-varying path loss, power delay profiles, delay and Doppler spreads. We also study the impact of LOS on received signal strength against the non-LOS and identify important propagation mechanisms by performing directional analysis of incoming signals. Finally, in section IV we summarize the discussion and present the conclusion.

II. V2V MEASUREMENT SETUP

V2V channel measurements were conducted using the RUSK Lund channel sounder that performs multiple-input multiple-output (MIMO) measurements based on the switched-array principle [6]. For the measurements, two standard hatch-back style cars were used and the four-element



Fig. 1. Aerial image of the investigated merging lane scenario outside city of Lund when the TX enters the highway while RX is approaching the merging point on the highway. (N $55^{\circ}42'36''$, E $13^{\circ}8'53''$)

antenna arrays were mounted on the roof. The height of each antenna array was 1.73 m from the ground. The channel sounder sampled the 4×4 MIMO time-varying channel transfer function H(f,t) over a 240 MHz of measurement bandwidth centered at 5.6 GHz, the highest allowed center frequency of the sounder. The temporal sampling and the measurement duration were set to $307.2 \,\mu s$ and $20 \, s$, respectively, with the test signal length of 3.2 μ s. The 4 × 4 MIMO antenna arrays were used to exploit diversity as the different TX-RX pairs give rise to different directional links. These arrays were designed specifically for V2V communication [7]. Each element of the arrays has a directional antenna gain such that the antenna pattern of element 1, 2, 3 and 4 have their main gain pointing to the left-side, backward, forward and to the right-side of the car, respectively. In the subsequent analysis we consider all four elements of the TX array such that the transmitter has somewhat omni-directional gain and then the power received at the element-1 is compared against the element-2 of the RX array.

To keep track of the positions of the transmitter (TX) and receiver (RX) cars, during the measurements, each vehicle logged the GPS coordinates and videos were recorded through the windshield. These data were also combined with the measurement data, in order to identify the important scatterers in the post-processing.

A. Scenario Description

The merging lane scenario at a highway is characterized as when the roads intersect at a certain angle, e.g., entrance or exit ramps. An important aspect of this scenario is the possibility of an obstructed LOS path due to the slope and the orientation of the terrain, or the presence of sound barriers, buildings or trees between the intersecting roads. This scenario is similar to the urban street crossings scenario [8], but with slightly more difficult channel conditions in the absence of LOS due to open surroundings, availability of fewer scatterers and higher vehicle speed. In order to draw conclusions on the importance of scatterers in the absence of LOS, the measurements were conducted for two types of scenarios: Sc-1) Vehicles merging

at an entrance ramp, when the RX car was driving on the highway and the TX car was entering on the highway; Sc-2) Vehicles splitting at an exit ramp, where the RX car was exiting from the highway and the TX car continued driving on the highway. In this paper we focus mainly on the merging lane situation (see Fig. 1), Sc-1, since this is the most important case in terms of collision avoidance and the experiences learned from these results can be applied on Sc-2. During each measurement RX car was moving on the highway and the TX car was entering on the highway from an entrance ramp. Both the cars were moving at the speed of $20-28\,\text{m/s}$ ($70-100\,\text{km/h}$). Two measurements are chosen for the analysis;

Sc-1*a*: when the TX enters the highway and remains behind the RX, which is already driving on the highway, and there are other vehicles driving by.

Sc-1*b*: when the TX enters the highway and remains in front of the RX, which is already driving on the highway, and there are no vehicles around.

III. DATA EVALUATION AND RESULTS ANALYSIS

To analyze the channel properties the data evaluation is performed as follows;

A. Averaged Power Delay Profile

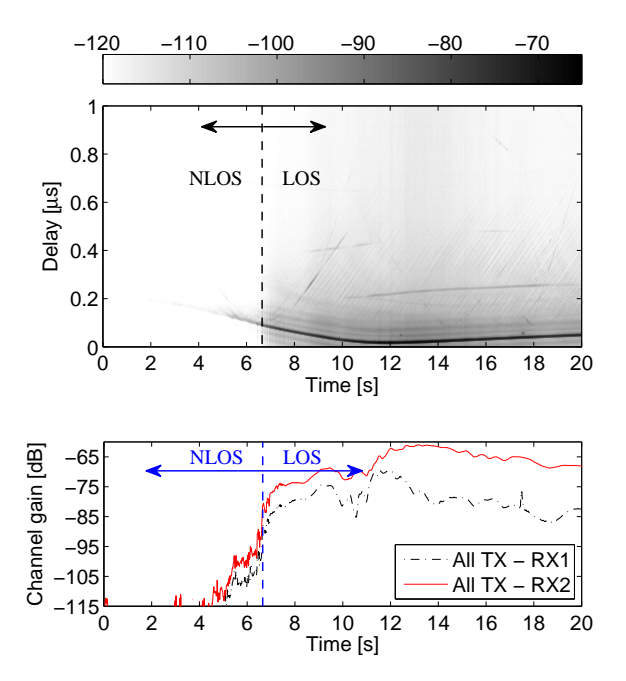
To analyze the impact of the absence of LOS and the time variations on the received signal power, the time-varying instantaneous power-delay-profile (PDP) is derived for each time sample. The averaged-PDP (APDP) reads,

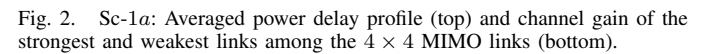
$$P_h(t_k, \tau) = \frac{1}{N_{avg}} \sum_{n=0}^{N_{avg}-1} |h(t_k + n\Delta t, \tau)|^2,$$
 (1)

for $t_k=\{0,N_{avg}\Delta t,...,\lfloor N_t/N_{avg}-1\rfloor\,N_{avg}\Delta t\}$, where $h(t_k+n\Delta t,\tau)$ is the complex time varying channel impulse response derived by an inverse Fourier transform of a channel transfer function H(f,t) for single-input single-output (SISO) antenna configuration and N_{avg} is the number of time samples used for averaging the effect of small-scale fading. The $N_{avg}=64$ is calculated as $N_{avg}=\lceil\frac{s}{v\Delta t}\rceil$, where $\Delta t=307.2\mu\,\mathrm{s}$ is the time spacing between snap shots, s= corresponds to the movement of TX and RX by 10 wavelengths and v is the velocity of TX and RX, $28\,\mathrm{m/s}$, approximately.

We also derive the time varying channel gain, by $G(t) = \sum_{\tau} P_{\tau}(t,\tau)$ where we apply a noise threshold, setting all components within $3\,\mathrm{dB}$ of the noise floor to zero.

The time-varying APDP and the corresponding channel gain are shown in Fig. 2 (Sc-1a) and in Fig. 3 (Sc-1b). From the APDP it is found that the channel is very poor in terms of scattering. It can be observed in both of the measurements that in the absence of LOS there are very few scattering objects that can provide additional propagation paths. Even if there are some moving objects close to TX/RX, their contribution seem to appear only when the LOS is available (see Fig. 2). It can be observed that the channel gain is higher in Fig. 2 than in Fig. 3 due to the additional power received from the MPCs,





reflected from the vehicles moving next to the TX/RX, and the difference in the gain of the RX element-1 and element-2 in different directions, e.g., in the forward and backward direction. This can be best appreciated in the plots of the channel gain in Fig. 2 and 3, where we show that the different TX-RX antenna pairs result in different channel gains due to different directional properties. The overall channel gain is higher in Sc-1a; when the RX is driving next to the TX, because the antenna gain of the RX is higher in the backward direction as compared to the forward direction. In addition to that, the number of scatterers also improve the channel gain in Sc-1a. For both of the measurements Sc-1a and Sc-1bthe channel gain for all TX-RX1 is $5-15\,\mathrm{dB}$ lower than the all TX-RX2 link because the main gain of RX element-1 is pointing in the direction opposite to the direction of the TX. The propagation mechanism driving these differences in gain can be well understood by performing a directional analysis of the measurement data.

B. Directional Analysis

For the characterization of antenna-channel interaction, a directional analysis, similar to [9], is performed using SAGE [5]. It is assumed that the 4×4 channel matrix H can be described by a sum of L plane waves or multi-path components (MPCs) where each wave l is characterized by a complex amplitude γ_l , propagation delay τ_l , Doppler shift ν_l , DOD and DOA, respectively, for both the azimuth and the elevation angles. The parameters for 100 MPCs are estimated from measured channel matrices and the DOA against the DOD for each MPC is presented in Fig. 4 and 5 for selected snapshots. The snapshots in Sc-1a; at time instant 10.58 s (top) and 17.56 s (middle), and in Sc-1b; at time instant 13.51 s (top)

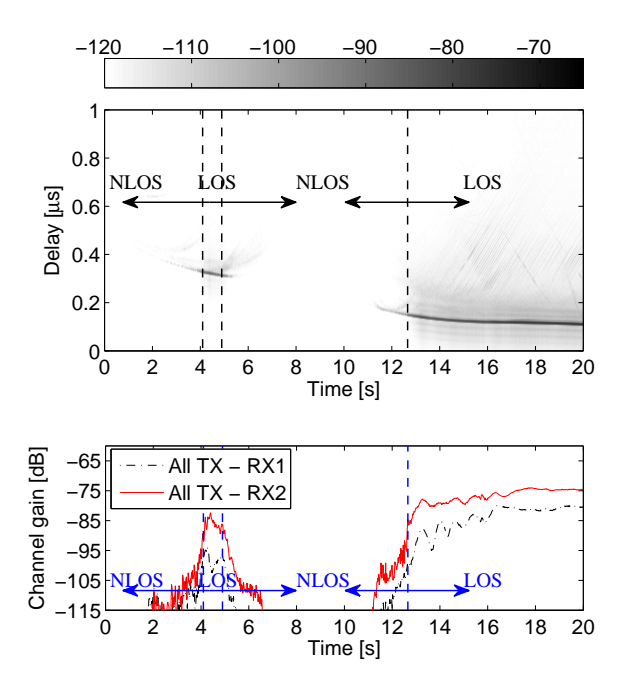


Fig. 3. Sc-1b: Averaged power delay profile (top) and channel gain of the strongest and weakest links among the 4×4 MIMO links (bottom).

and 17.56 s (middle), are chosen as example for the analysis. MPCs with power 20 dB less than the LOS component have not been shown. The propagation delay τ_l of each MPC is normalized by the propagation delay of the LOS component τ_{LOS} such that LOS has $\tau_{LOS}=0$ s delay. The delay τ_l is shown as the propagation distance $S_l=c\times(\tau_l-\tau_{LOS})$ in the color bar in Fig. 4 and 5.

In the merging lane scenario there are very few interacting objects often widely separated in space which results in very few reflected propagation paths in addition to the LOS component. Due to the sparsity of interacting objects, the propagation distances of these MPCs are large and the signal strength is usually very low. Moreover, 3-7 MPCs with power $10 - 20 \,\mathrm{dB}$ lower than the LOS component are seen in Fig. 4 and 5. These MPCs with 1-3 m longer propagation distance relative to LOS propagation distance are the paths originating from the single bounce reflection with the road sign and the metallic guard rail between the ramp and the highway, and the ground reflections. Most of these MPCs are available only when there is LOS. Therefore, the received power is negligible in the absence of LOS (as shown in Fig. 2 and 3) and the LOS component constitutes most of the received power when there is a LOS between TX and RX (see Fig. 4 and 5).

To analyze the variations in the received power due to the variation in the antenna gain it is important to analyze the power variations in the LOS component. The vertical dotted lines are drawn to visualize the DOA of the LOS component, the largest circle, for each snapshot to compare the differences in the antenna gain for RX element-1 and element-2 at that particular angle. As a first observation it is found that the received power can drop up to 20 dB depending upon the DOA and the differences in the antenna gain of the RX elements

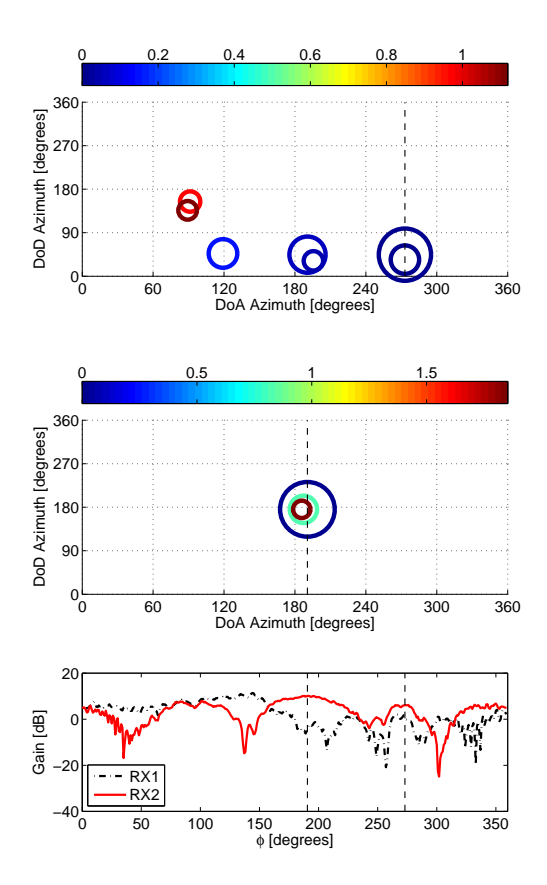


Fig. 4. Sc-1a: The azimuth direction-of-arrival (DOA) and azimuth direction-of-departure (DOD) estimates for the snapshots at time instant $10.58\,\mathrm{s}$ (top) and $17.56\,\mathrm{s}$ (middle), and the azimuth antenna gain of RX element-1 and element-2 (bottom) are shown. The color bar is representing the relative distance (m) w.r.t the LOS component such that the LOS component is at 0 m. The size of the circles depicts power carried by each MPC.

at that angle. Comparing these results with the channel gain results in Fig. 2 (Sc-1a) and in Fig. 3 (Sc-1b), we find a direct correlation between the channel gain and the antenna radiation pattern. This implies that, even if there is a LOS between the TX and RX, the power level can drop significantly when there is a dip in the antenna pattern. This can have severe impact on the communication range and thus it needs to be considered when designing an antenna for auto-motive safety applications.

C. Delay and Doppler Spreads

The root mean square (rms) delay and Doppler spreads are also important parameters in system design. As they describe how the power is spread by the channel in time and in frequency, and they are good indicators of the frequency selectivity (rms delay spread) and the time selectivity (rms Doppler spread) of the channel. Moreover, they can be related to the coherence bandwidth and coherence time as described in [10]. We calculate the time-varying rms delay and Doppler spreads as in [11] applying a threshold on the data such that we can avoid erroneous results due to spurious components. We set all components below the noise floor plus 3 dB (*noise thresholding*) to zero.

The time-varying rms delay spread and rms Doppler spread for the first scenario (Sc-1a) are shown in Fig. 6. We plot

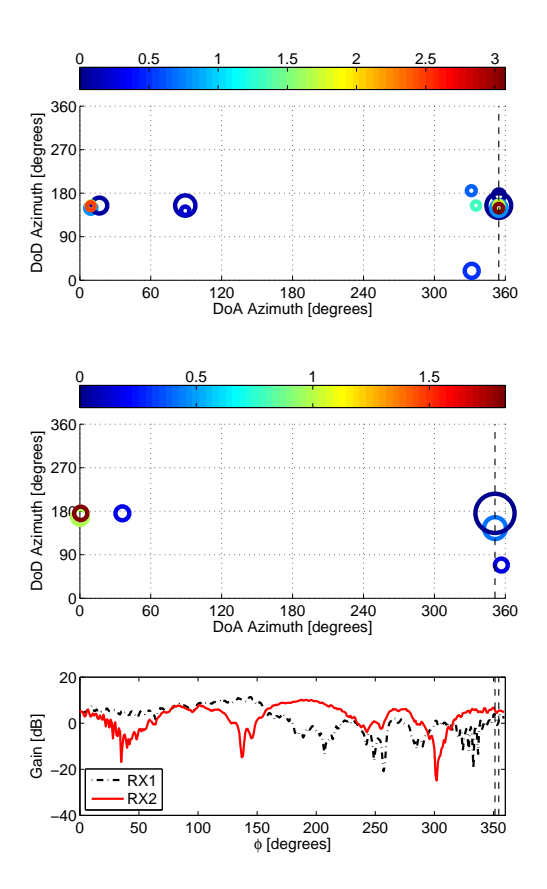


Fig. 5. Sc-1b: The azimuth direction-of-arrival (DOA) and azimuth direction-of-departure (DOD) estimates for the snapshots at time instant 13.51s (top) and 17.56s (middle), and the azimuth antenna gain of RX element-1 and element-2 (bottom) are shown. The color bar is representing the relative distance (m) w.r.t the LOS component such that the LOS component is at 0 m. The size of the circles depicts power carried by each MPC.

the results for three different configurations, as similarly done in the previous section: in green dotted line we show the rms spreads when considering all TX antennas and all RX antennas; in red dashed line we show the results obtained when considering all TX antennas and only RX element-1; and in black solid line we consider all TX antennas and only RX element-2.

First we observe that the rms spreads are not equal for the three links, mainly observable in the rms delay spread plot (Fig. 6 top). The link between all TX antennas and RX element-2 is the most frequency selective one, since many strong MPCs are visible which contribute to a large rms delay spread. The antenna element 2 is focusing towards the TX (RX driving in front of the TX), therefore, the surrounding scatterers are illuminated the most, thus resulting in strong MPCs at the RX. On the other hand, when considering all RX antennas, the power of the LOS and all other MPCs is averaged over all RX antennas. Often all scatterers do not contribute to the power received at each RX antenna therefore the averaged power of scatterers over all RX antennas can be lower than their power in each link. Moreover, the power of the LOS component is much larger than the power of the later MPCs, so the rms delay spread is small. This difference between links observed in the rms delay spread is not as remarkable in the

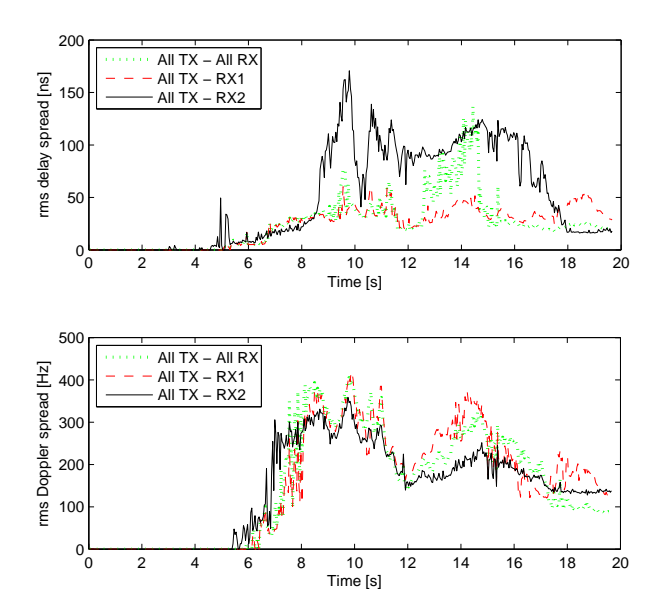
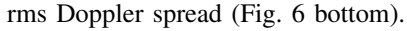


Fig. 6. Sc-1a: Time-varying rms delay spread (top) and time-varying rms Doppler spread (bottom) for scenario 1.



In Fig. 7 we depict the time-varying rms delay and Doppler spread for the second scenario (Sc-1b). Here we observe a similar behavior, but since now the TX is driving in front of the RX, the RX element-2 is not focusing on the TX anymore, the number of illuminated objects is smaller than it is for the other links. Therefore, the link all TX - RX2 shows the smallest rms delay spread compared to the other links.

Noteworthy is the different curves of the time-varying rms Doppler spread in Fig. 7 in the bottom. The highest values are obtained for the link between all TX antennas and RX element-2 at 5 s. This might be originated by a reflection on a metallic object left behind the TX, probably a metallic fence on the side of the road. A similar effect caused by the reflections on the fence separating the two lanes of the road is observed between 14 and 16 s, and it drops when the TX and the RX are aligned.

IV. SUMMARY AND CONCLUSIONS

This paper presents results from a vehicle-to-vehicle measurement campaign for the safety applications targeting collision avoidance in merging lanes. Looking at the results from different measurements, we found that the channel gain is highly dependent on the line-of-sight (LOS) in such a sparse scenarios. Due to lack of significant scatterers such as road side objects and vehicles the received power decays abruptly in the absence of LOS which demonstrates the importance of LOS. Moreover, the antenna radiation pattern plays an important role due to the fact that there are few scatterers and if the antenna has a poor gain in the direction of TX the received power level can drop significantly. Thus designing an antenna that has an omni-directional gain, or using multiple antennas radiating towards different directions becomes more important for such a safety critical scenarios.

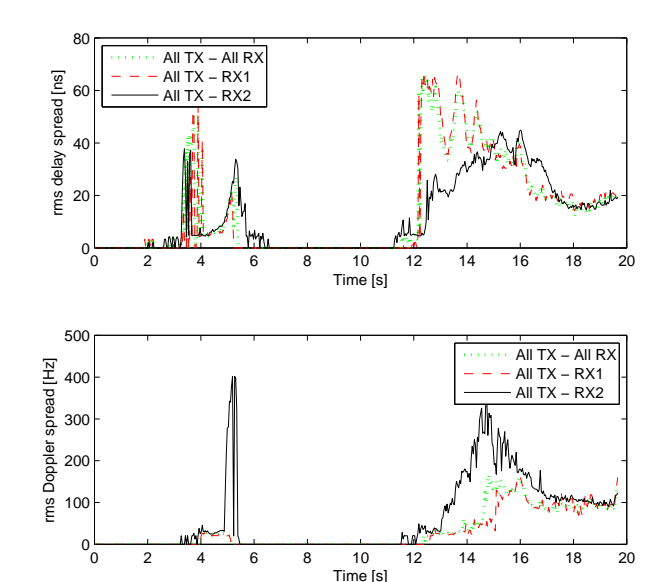


Fig. 7. Sc-1b: Time-varying rms delay spread (top) and time-varying rms Doppler spread (bottom) for scenario 2.

REFERENCES

- [1] T. Sakaguchi, A. Uno, and S. Tsugawa, "Inter-vehicle communications for merging control," in *Vehicle Electronics Conference (IVEC '99) Proceedings of the IEEE International*, 1999, pp. 365 –370 vol.1.
- [2] A. Uno, T. Sakaguchi, and S. Tsugawa, "A merging control algorithm based on inter-vehicle communication," in *Intelligent Transportation Systems. Proceedings of the IEEE/IEEJ/JSAI International Conference* on, 1999, pp. 783 –787.
- [3] Q. Xu and R. Sengupta, "Simulation, analysis, and comparison of ACC and CACC in highway merging control," in *Intelligent Vehicles* Symposium, 2003. Proceedings. IEEE, june 2003, pp. 237 – 242.
- [4] Y. Liu, U. Ozguner, and T. Acarman, "Performance evaluation of intervehicle communication in highway systems and in urban areas," in *Intelligent Transport Systems, IEE Proceedings*, vol. 153, no. 1, march 2006, pp. 63 75.
- [5] B. H. Fleury, M. Tschudin, R. Heddergott, D. Dahlhaus, and K. I. Pedersen, "Channel parameter estimation in mobile radio environments using the SAGE algorithm," *IEEE J. Select. Areas Commun.*, vol. 17, no. 3, pp. 434–450, Mar. 1999.
- [6] R. Thoma, D. Hampicke, A. Richter, G. Sommerkorn, A. Schneider, U. Trautwein, and W. Wirnitzer, "Identification of time-variant directional mobile radio channels," *Instrumentation and Measurement, IEEE Transactions on*, vol. 49, no. 2, pp. 357 –364, apr 2000.
- [7] A. Thiel, O. Klemp, A. Paier, L. Bernadó, J. Karedal, and A. Kwoczek, "In-situ vehicular antenna integration and design aspects for vehicle-tovehicle communications," in *EUCAP*, Apr. 2010.
- [8] J. Karedal, F. Tufvesson, T. Abbas, O. Klemp, A. Paier, L. Bernadó, and A. F. Molisch, "Radio channel measurements at street intersections for vehicle-to-vehicle safety applications," in *IEEE VTC 71st Vehicular Technology Conference (VTC 2010-spring)*, May 2010.
- [9] T. Abbas, J. Karedal, F. Tufvesson, A. Paier, L. Bernado, and A. Molisch, "Directional analysis of vehicle-to-vehicle propagation channels," in 2011 IEEE 73rd Vehicular Technology Conference (VTC Spring), may 2011, pp. 1 –5.
- [10] A. F. Molisch and M. Steinbauer, "Condensed parameters for characterizing wideband mobile radio channels," *International Jour*nal of Wireless Information Networks, vol. 6, pp. 133–154, 1999, 10.1023/A:1018895720076.
- [11] L. Bernadó, T. Zemen, A. Paier, G. Matz, J. Karedal, N. Czink, F. Tufvesson, M. Hagenauer, A. F. Molisch, and C. F. Mecklenbräuker, "Non-WSSUS Vehicular Channel Characterization at 5.2 GHz Spectral Divergence and Time-Variant Coherence Parameters," in Assembly of the International Union of Radio Science (URSI), August 2008, pp. 9–15.